Jordan Journal of Physics

ARTICLE

Influence of Solvents on Properties of ZnS Thin Films Synthesized by Chemical Spray Pyrolysis Technique

Akintunde A. Ajayi[a], **Aderemi B. Alabi**[b], **Olutayo W. Abodunrin**[a], **Ibukun S. Akinsola**[b,c], **Olukunle C. Olawole**[d], **Abiodun M. Salawu**[b] and **Adewale Ayeni**[b]

[a] *Department of Mathematical and Physical Sciences, Afe Babalola University, Ado-Ekiti, Nigeria.*

[b] *Department of Physics, University of Ilorin, Ilorin, Nigeria.*

[c] *Department of Physical and Mathematical Sciences, Crown-Hill University, Ilorin, Nigeria.*

[d] *Department of Physics, Covenant University, Ota, Nigeria.*

Abstract: In this paper, the influence of solvents on the structural, optical, surface and electrical properties of spray-deposited ZnS thin films has been studied. Different precursor mixtures were prepared from ethylene glycol, deionized water and alcohol solvents and sprayed on heated glasses *via* a simple and cost-effective technique known as spray pyrolysis. XRD patterns confirmed cubic and tetragonal phases of synthesized ZnS material. The optical analysis of the synthesized ZnS films showed that films prepared using ethylene glycol solvent have the highest transmittance and the best bandgap (3.61 eV). Surface morphology showed the absence of voids and pinholes in the Scanning Electron Micrograph of ZnS film prepared from ethylene glycol and electrical studies showed that ZnS films prepared using the same solvent have the lowest resistivity.

Keywords: ZnS, Thin film, Spray pyrolysis, Bandgap, Morphology.

Introduction

Zinc sulfide is a group II-VI chalcogenide compound with semiconducting properties. It finds applications as an n-type partner in heterojunction solar cells [1], UV light emitting diodes [2] and as a photoanode in photoelectrochemical water splitting [3]. The aforementioned applications are as a result of ZnS wide bandgap of about 3.70 eV which is the highest among chalcogenide semiconductors [4]. The constituents of ZnS are ecofriendly and abundant and can be a possible replacement for cadmium sulfide which is an n-type partner in commercialized thin-film solar cells, such as Copper Indium Gallium Selenide (CIGS) and Cadmium Telluride (CdTe) solar cells [5]. It can also be used as a buffer layer in a smart absorber material like Copper Zinc Tin Sulfide (CZTS) [1].The techniques used in the synthesis of ZnS thin films in most reported works are wet chemical technique which includes spray pyrolysis [6, 7], chemical bath deposition [5, 8], successive ionic layer and reaction (SILAR) [9, 10], chemical vapor deposition (CVD) [11, 12] and sol-gel [13-15]. Among the fore-named chemical methods, spray pyrolysis stands out as a simple technique for low-cost deposition [16]. It is applicable over a wide area, industrially scalable and stoichiometry can be easily controlled. It is well known that deposition parameters in spray pyrolysis play a significant

---

Corresponding Author: Olutayo Wale Abodunrin   **Email**: tayoabodunrin@yahoo.com

role in enhancing structural and opto-electronic properties of the final product [16]. One of the deposition parameters is the type of solvent used in preparing starting precursor solution which can be correlated to behavior of the evaporating solution [17]. The use of deionized, distilled or double distilled water in preparation of precursor mixture containing zinc salt and thiourea has been reported in most works on ZnS thin films, though complexing agents are sometimes added to enhance the stability of the solution [18-21]. The effect of solvent on properties of ZnS has not been adequately investigated, though, in 2018, Liu et al. investigated the effect of solvents on spin-coated ZnS films [41]. The aim of this study is to investigate the effect of solvent on properties of ZnS thin films deposited by spray pyrolysis technique with an objective to correlate properties of ZnS thin film to solvent properties.

Experimental Details

Precursor solutions containing 0.025 M of zinc acetate dihydrate $(ZnC_4H_6O_4.2H_2O)$ and 0.2 M of water-soluble organic compound thiocarbamide $(CS(NH_2)_2)$ were prepared with solvents; ethylene glycol, deionized water and alcohol. All reagents are analytical grade and were purchased from Sigma Aldrich. The high concentration of thiocarbamide will compensate for sulphur loss during pyrolysis. Each solution was stirred continuously for an hour until a clear solution was obtained without addition of any complexing agent except for the solution prepared with deionized water in which a drop of H_2SO_4 was added to prevent precipitation in the mixture. The solution was sprayed on soda-lime glasses heated to $400^{\circ}C$ at the rate of 2mL/minute. The spray assembly is shown in Fig. 1. Air was used as the carrier gas at a pressure of 40 psi. Spray to target distance was maintained at 25 cm. The resulting ZnS thin films were classified as specimens ZG, ZA and ZD, where ZG represents sprayed ZnS thin film sample obtained from ethylene glycol, ZA represents sprayed thin film specimen obtained from alcohol and ZD represents sprayed thin film specimen obtained from deionized water. ZG, ZD and ZA were annealed in a muffled furnace at $300^{\circ}C$ for one hour. Weight of the films and substrates was measured using Adventurer balance (model: Adventurer Pro AV313 d = 0.0001g.
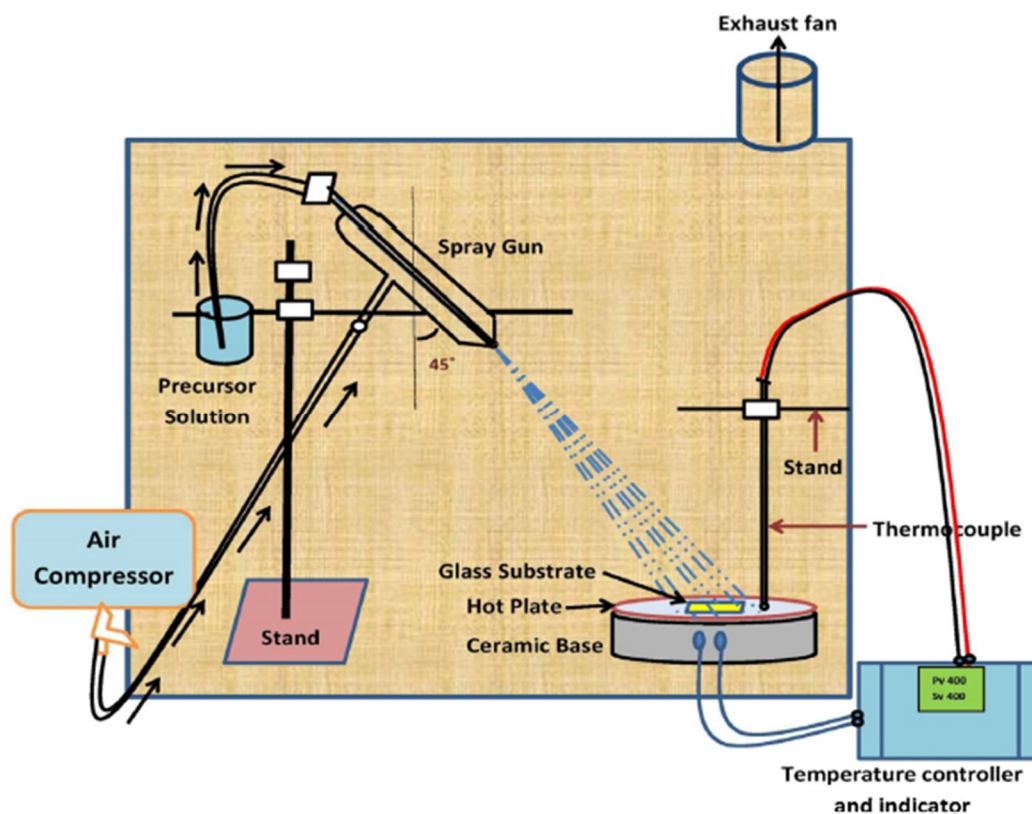
FIG. 1. Schematic diagram of experimental spray pyrolysis assembly [38].

Characterization of ZnS Thin Films

The structural characterization of the samples was done using a Rigaku D/Max-IIIC X-ray diffractometer with a lynx eye detector using a copper target *(Cuα, 1.5418 Å)*. All X-ray diffraction (XRD) data for the specimens was recorded at current and acceleration voltage of 25mA and 40 kV, respectively. Surface morphology and grain growth analysis of CZTS samples were carried out by using Hitachi scanning electron microscope (SEM) and optical characterization was done using UV-Vis spectrophotometer of CyberLab (model no. UV-100).

Results and Discussion

Structural Properties

The XRD patterns of ZG, ZD and ZA are shown in Figs. 2, 3 and 4, respectively. The pattern of ZG shows diffraction peaks corresponding to (111), (220) and (311) reflection planes of cubic ZnS which are observed at 2θ equaling 28.6°, 48.1° and 57.2°. The peaks matched well with the Crystallography Open Database; American Mineralogist Crystal Structure Database (COD-AMSCD) with Card no. 96-500-5089. The broadening observed at the peaks is an evidence of the nanocrystaline nature of the specimen. There was no evidence of secondary phase in the specimen. Grain size was calculated using Eq. 1and 2.67 nm was obtained as the grain size of ZD. This result is in agreement with earlier works [20-23] The pattern of ZD shows diffraction peaks at 2θ equaling 30.9°, 33.0°, 48.1°, 56.5° and 69.5° which can be indexed to (101), (200), (220), (112) and (400) respective reflection planes which are the planes of cubic and hexagonal structure of ZnS. However, some peaks corresponding to zinc oxide (ZnO) are observed at 2θ equaling 35.6° and 35.4°. The presence of oxides of zinc can be attributed to decomposition of microsized droplets of precursor mixture during open air spraying. The calculated grain size for ZD is 66.0 nm. The pattern of ZA shows peaks at 2θ equaling 28.1⁰, 30.4⁰ and 33.6⁰ which can be indexed to (111), (101) and (200) reflection planes of cubic and hexagonal phases of ZnS respectively. Other peaks that cannot be indexed to planes of ZnS were observed in the diffractogram of ZA. A grain size of 264.8 nm was obtained for ZA. The results are in agreement with works that have reported cubic and tetragonal crystal structure of ZnS [23] [24]. Variation in grain size from crystalline in ZA and ZD to nanocrystalline in ZG due to solvent influence can be explained by taking the polarity and vapor pressure of the solvents into account. Slower evaporation rate induced by lower vapour pressure may have been responsible for small grain size of ZG (see Fig. 5). Correlation between grain size and vapour pressure has been reported in a very recent work [36]. Increase in grain size with corresponding decrease in polarity can be observed in Fig. 6. It can be suggested that a reduction in solvent polarity causes loose coiling of bonds, which results in higher aggregate formation. The consequence of this is formation of smaller aggregates during drying of specimen prepared using solvent with higher dipole moment. Liu et al. [41] reported a small intensity peak for ethylene glycol against ethanol. We have succeeded in improving the structural properties of ZnS thin film synthesized using ethylene glycol by post-deposition annealing at 300°C and without the use of hydrazine which is toxic. Table 1 shows the polarities and vapour pressures of the solvents used in preparing the ZnS precursor solution.

$$G = \frac{0.9\lambda}{\beta cos\theta} \qquad (1)$$

where G is the grain size, λ is the CuK$_α$, β is the full width at half maximum and θ is the angle of diffraction.

TABLE 1. Dipole moments and vapour pressures of solvents [39] [40].

Solvent	Dipole Moment (Debye)	Vapour Pressure (kPa)
Alcohol	1.660	5.950
Water	1.850	2.400
Ethylene Glycol	2.747	0.007
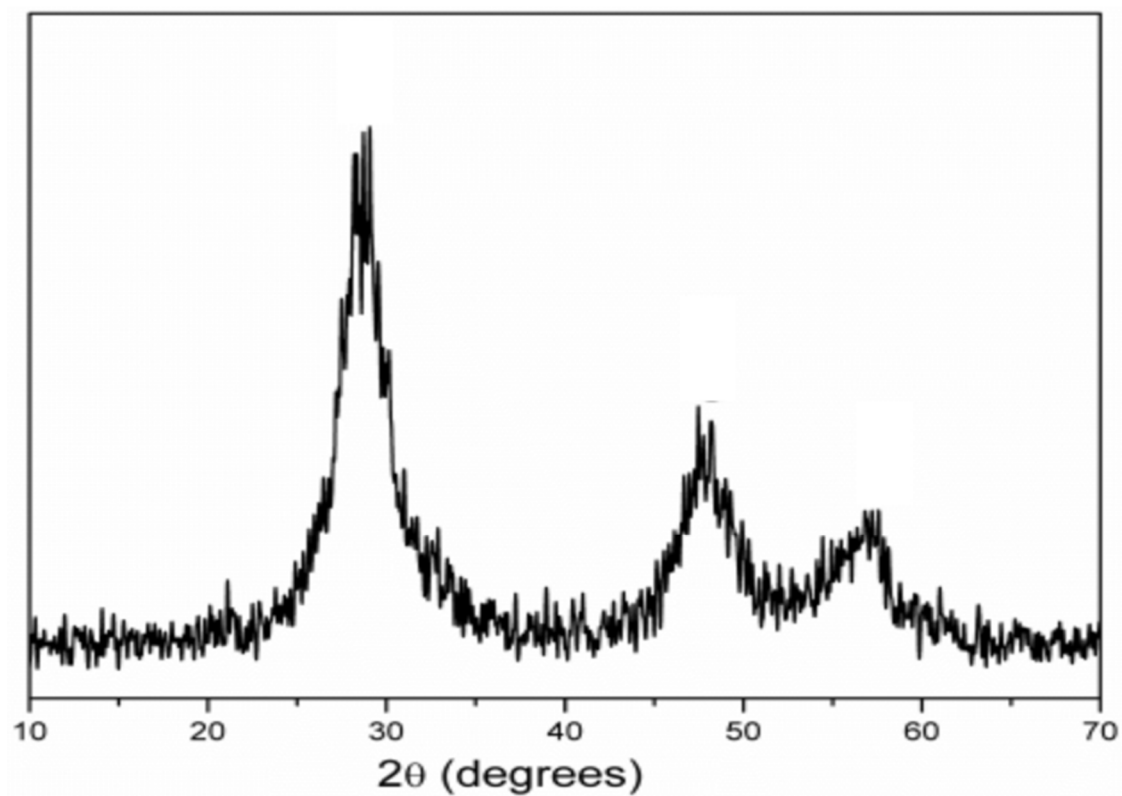
FIG. 2. XRD patterns for ZnS thin films prepared using ethylene glycol solvent.
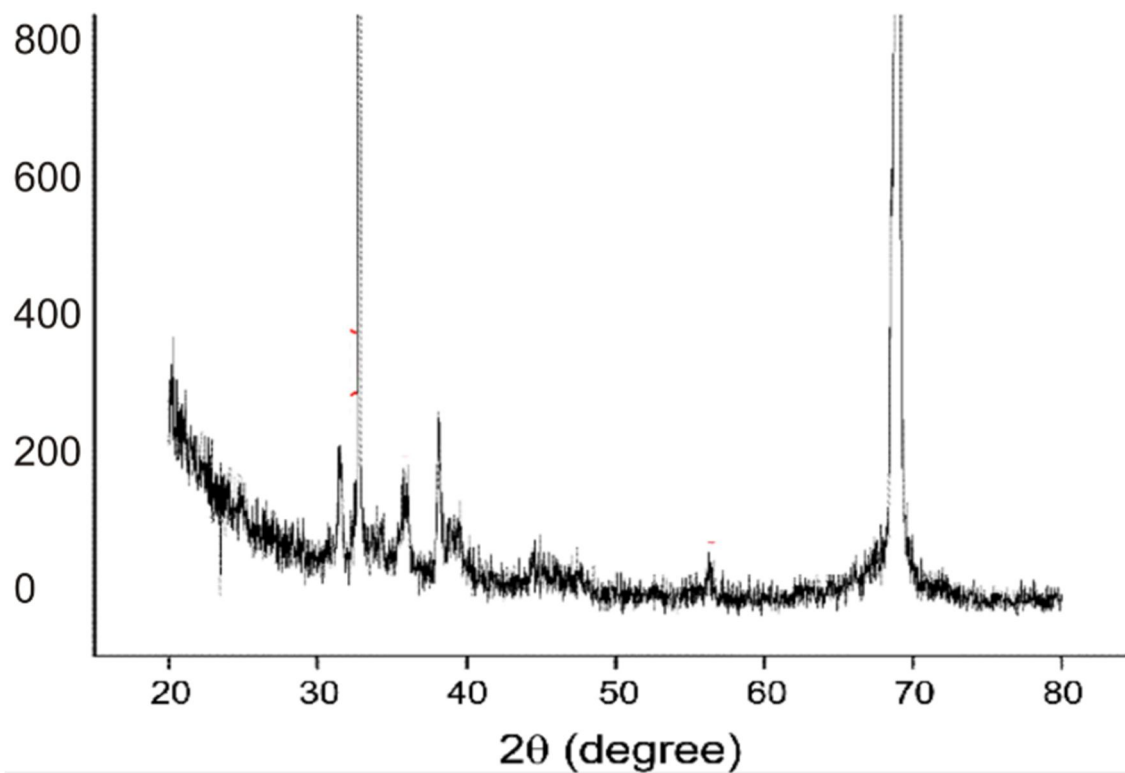
FIG. 3. XRD patterns for ZnS thin films prepared using deionized water solvent.
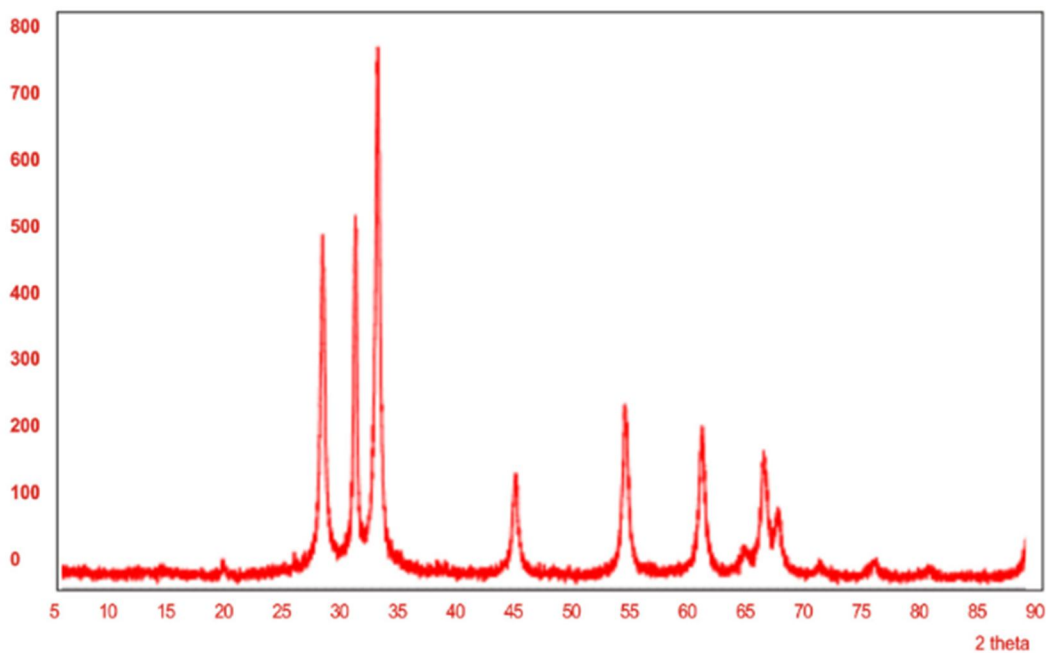
FIG. 4. XRD patterns for ZnS thin films prepared using alcohol solvent.
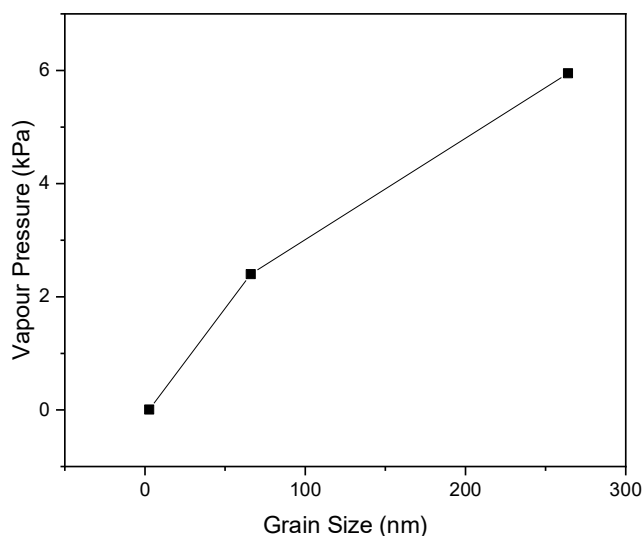
FIG. 5. Plot of vapour pressure of solvents *versus* Grain size of ZnS thin films.
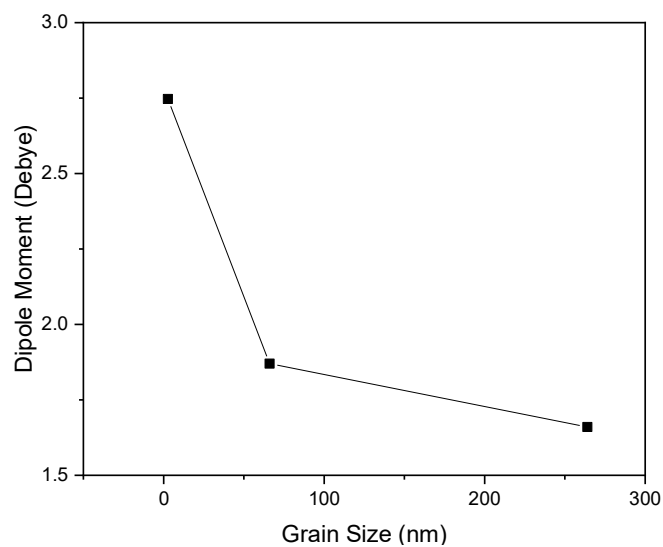
FIG. 6. Plot of dipole moment *versus* grain size of sprayed ZnS thin films.

353

Optical Properties

Transmission and absorption spectra of samples ZG, ZD and ZA are shown in Figs. 7 and 8. Transmission data was obtained from ultraviolet-visible spectroscopy measurements and the absorbance of the films was calculated using the equation:

$$A = 2 - log(T\%) \qquad (2)$$

Highest transmittance and lowest absorbance can be observed in ZG within the ultraviolet-visible region, while the lowest transmittance and highest absorbance can be observed in specimen ZA. The increase in slope of the transmittance curve of ZD may be a result of drying retardation during decomposition of ZnS precursor due to solvent type. The smoothness of

the absorption spectra is an evidence of homogeneity in all the specimens. It can be observed that the absorption edge is redshifted with decreasing solvent polarity as expected of a window layer in thin-film solar cell. The optical bandgap of the spray-deposited ZnS thin films was calculated from the Tauc plot. The plot is derived from the expression:

$$(\alpha hf)^{1/n} = A(hf - E_g) \qquad (3)$$

where α is the absorption coefficient, h represents Planck's constant, f represents photon frequency, E_g represents the energy band-gap and A is a constant of proportionality. n depends on the nature of radiative transition and is given as n = ½ for directed allowed band-gap.
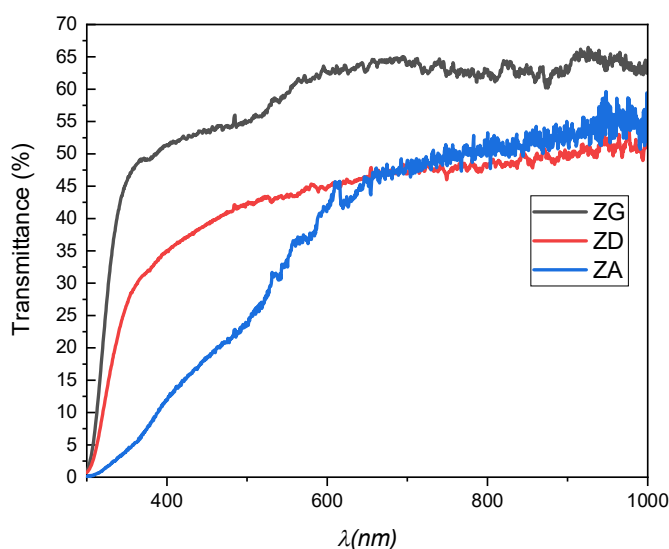
FIG. 7. Variation of transmission spectra of ZnS thin films with solvents of ethylene glycol, deionized water and alcohol.
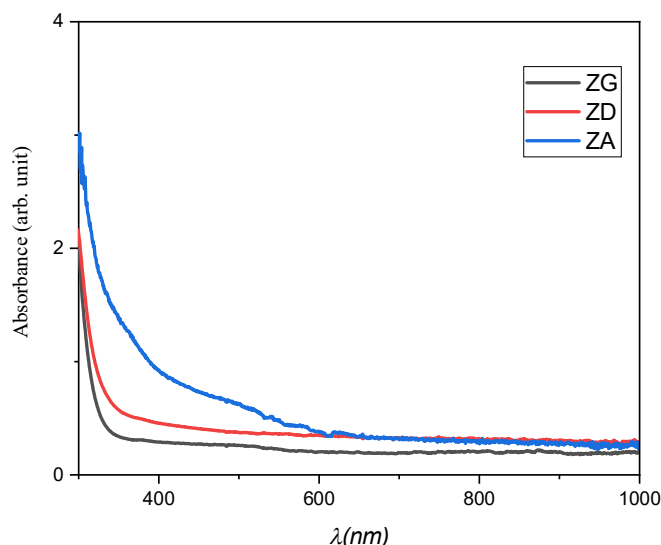
FIG. 8. Variation of absorption spectra of *ZnS* thin films with solvents of ethylene glycol, deionized water and alcohol.

Fig. 9 shows the plot of $(\alpha hf)^2$ *versus* hf. The bandgap E_g is obtained from the intercept with axis hf after extrapolating the linear region of the plot. Fig. 9 shows the Tauc's plot for ZG, ZD and ZA, where a superior bandgap of 3.61 eV can be observed in ZG, while ZD and ZA showed lower energy bandgaps of 3.56 eV and 3.38 eV, respectively. The bandgap is not widely influenced by solvent variation and matches those frequently reported in literature [25-28]. This is an indication that bond length and quinoidal character (higher energy state due to replacement of single bonds with double ones) have not been affected by solvent type.
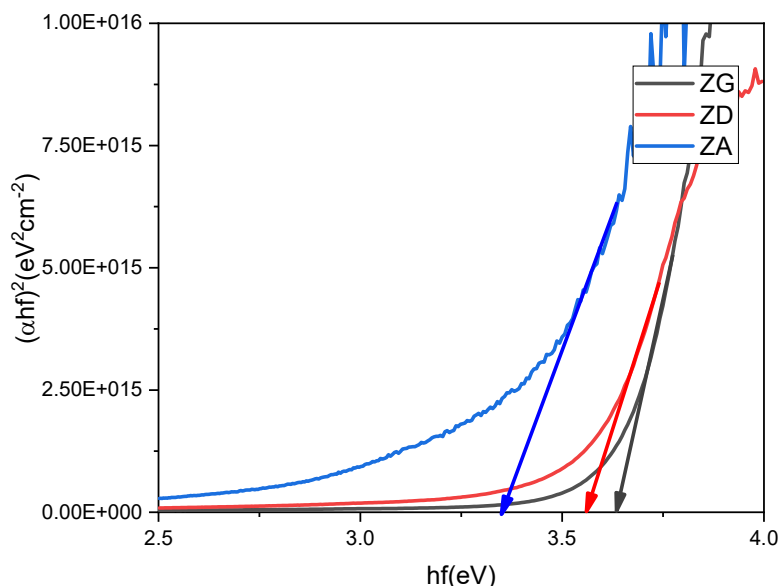
FIG. 9. Variation of optical bandgap of ZnS thin films with solvents of ethylene glycol, deionized water and alcohol.

Morphological Properties

The surface morphology of spray-deposited ZnS thin films was studied using scanning electron microscope. The scanning electron micrographs (SEM) of ZG, ZD and ZA are shown in Fig. 10. The surface morphology of the films is influenced by solvent variation to some extent, where ridges can be observed in ZnS thin films prepared using ethylene glycol as a solvent. Some voids can be seen in the SEM of ZG and ZA and the greater grain size of ZD is clearly confirmed by the SEM results. The ridges notwithstanding, it can be observed that ZG has a greater uniform surface morphology compared to the other two specimens. It has been reported in some research works on thin-film semiconductors that uniform surface morphology leads to less grain boundaries [29-31].
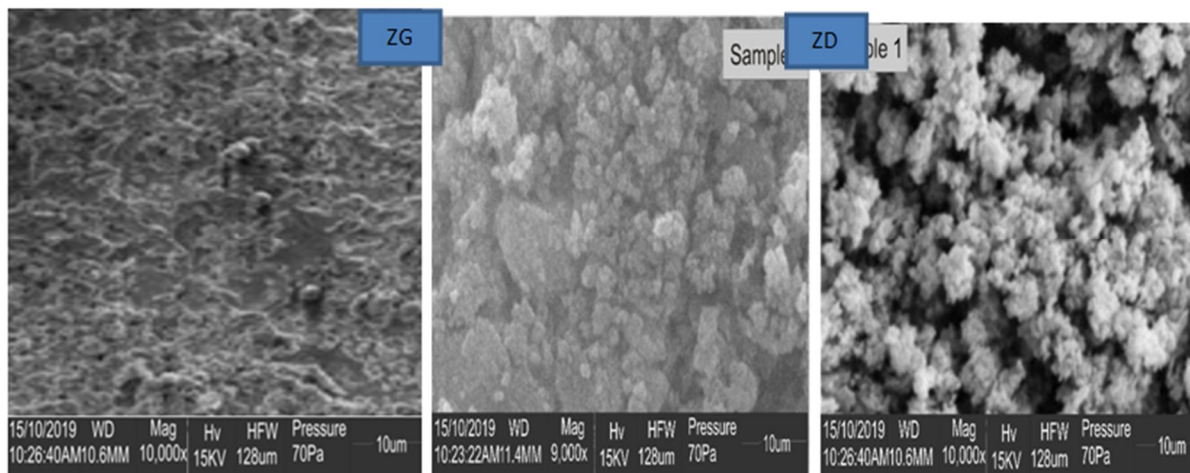
FIG. 10. SEM micrographs of ZG, ZD and ZA.

Compositional Analysis

The composition of the solvent-varied ZnS thin films was analyzed by energy dispersive X-ray spectroscopy (EDX). The EDX spectra of ZG, ZD and ZA are shown in Fig 11. The ZnS compound is confirmed by the peaks of zinc (Zn) and sulphur (S) in the EDX. It can also be observed that all synthesized films are highly Sulphur-deficient, which may be attributed to affinity of sulphur towards oxygen leading to formation of sulphur (IV) oxide which is lost during pyrolysis [33] [34]. However, the highest atomic percentage of sulphur can be found in specimen ZG, as shown in Table 2, which may be due to drying retardation during the spraying process. Oxygen peaks observed may be due to air used as carrier gas and the carbon peak may be attributed to C=O functional group in ZG.
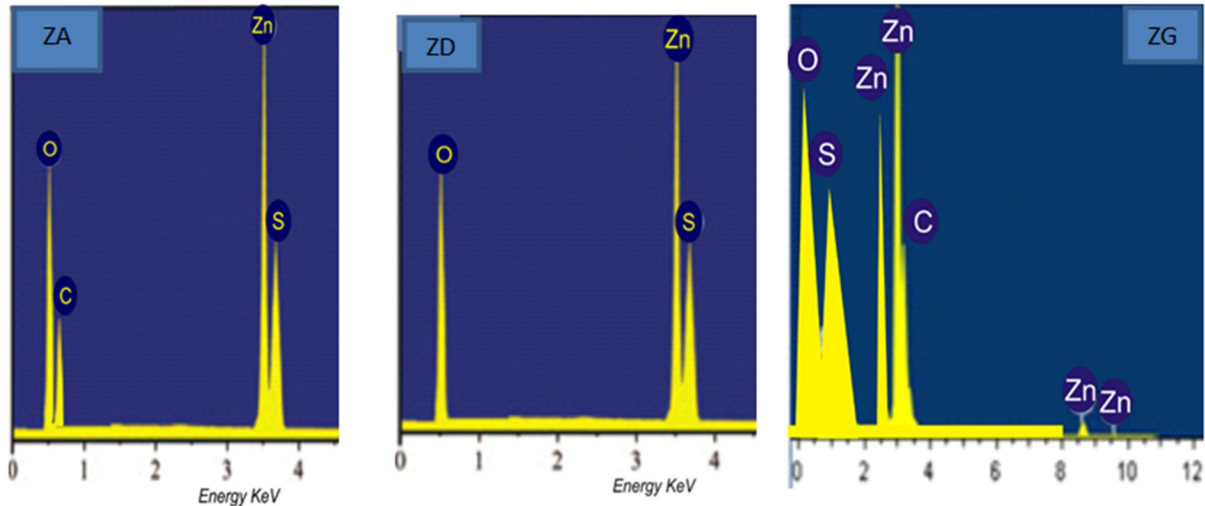
FIG. 11. EDX spectra of ZG, ZD and ZA.

TABLE 2. Elemental composition of solvent-varied ZnS thin films.

Specimen	Zn Atomic %	S Atomic %	O Atomic %	C Atomic %
ZG	50.46	15.75	20.50	7.22
ZD	60.29	9.25	30.46	-
ZA	68.00	7.60	20.00	4.40

Electrical Properties

Resistivity of solvent-varied ZnS thin films was obtained from current-voltage measurements carried out by a Keithley source meter instrument with Tracer software using Vander pauw array mode with indium pellet as ohmic contact. Resistivity was calculated using the following equation:

$$\rho = Rt \tag{4}$$

where ρ is resistivity, R is the sheet resistance and t is the thickness of the film. The thickness of the films was evaluated using the weight difference method [35] expressed as:

$$t = \frac{m}{dA} \tag{5}$$

where t is thickness, ρ is density of cubic phase of ZnS, equal to 4.1 gcm^{-3} [35], A is the area of the film and m is the mass of deposited films.

The resistivity values of ZG, ZD and ZA are shown in Table 3 with ZG observed to have the lowest value of resistivity.

TABLE 3. Resistivity of Solvent-varied ZnS thin films.

Specimen	ρ (x10^5)(Ω.cm)	t (μm)
ZG	2.47	0.25
ZD	74.28	0.75
ZA	35.66	0.34

Conclusion

In this study, ZnS thin films have been synthesized *via* a simple and cheap chemical technique: spray pyrolysis. The influence of solvents on the structural, optical, surface and electrical properties of spray-deposited ZnS thin films has been studied. Ethylene glycol, deionized water and alcohol are solvents used in preparation of the precursor mixture containing zinc salt and thiocarbamide. The films developed from precursor mixture with ethylene glycol used as solvent exhibited cubic phase of ZnS only, while those developed from deionized water and alcohol showed both cubic and tetragonal phases. It can be suggested from the small grain size (2.67 nm) of ZG that the film is nanocrystalline, while ZnS thin film synthesized from deionized water has the largest grain size of 264.80 nm. The ZnS thin film synthesized from ethylene glycol exhibited the highest percentage transmittance in the ultraviolet-visible region of the electromagnetic spectrum with a superior bandgap of 3.61 eV; though the effect of solvent type on sprayed ZnS thin film was not far-reaching. Voids and pinholes are absent in the surface of ethylene glycol-synthesized films. In the case of ZnS films prepared from deionized water and alcohol, some voids can be noticed though the particle sizes are more distinguishable compared to those of ethylene glycol. Evaluation of current-voltage characteristics of the films showed that ZnS thin film synthesized from ethylene glycol is less resistive (2.47×10^5 Ω.cm) compared to the large values of the resistivity of specimens ZD and ZA which are 74.28×10^5 Ω.cm and 35.66×10^5 Ω.cm, respectively.

References

[1] Boutebakh, F.Z., Beloucif, A., Aida, M.S., Chettah, A. and Attaf, N., Journal of Materials Science: Material in Electronics, 29 (2017) 4089.

[2] Kassim, A., Nagalingam, S., Min, H.S. and Karrim, N., Arabian Journal of Chemistry, 3 (2010) 243.

[3] Hassan, M.A., Johar, M.A., Waseem, A., Bagal, I.V., Ha, J. and Ryu, S., Optics Express, 27 (4) (2019) A184.

[4] Offor, P.O., Okorie, B.A., Ezekoye, B.A., Ezekoye. V.A. and Ezema, J.I., Journal of Ovonic Research, 11 (2) (2015) 73.

[5] Manjulavalli, T.E. and Kannan, A.G., International Journal of ChemTech Research, 8 (11) (2015) 396.

[6] Offor, P.O., Whyte, G.M., Otung, F.U., Nnamchi, P.S., Ude, S.N., Omah, A.D., Daniel-Mkpume, C.C., Neife, S.I., Aigbodun, V.S., Madu, S., Okorie, B.A. and Ezema, F.I., Surfaces and Interfaces, 16 (2019) 157.

[7] Djelloul, A., Adanne, M., Larbah, Y., Sahraoui, T., Zegadi, C., Maha, A. and Rahal, B., Journal of Nano-and Electronic Physics, 7 (4) (2015) 1.

[8] Liu, W., Chen, W., Hsieh, S. and Yu, J., Procedia-Engineering, 36 (2012) 46.

[9] Ashith, V.K. and Gowrish, R.K., IOP Conf. Series: Materials Science and Engineering, 360 (2018) 012058.

[10] Ates, A., Yildirim, M.A., Kundakci, M. and Astam, A., Materials Science in Semiconductor Processing, 10 (6) (2007) 281.

[11] Palve, A.M., Thin Solid Films, 6 (42) (2019) 1.

[12] Vishwakarma, R., Ukrainian Journal of Physics, 62(5), (2017) 422.

[13] Ahktar, M.S., Riaz, S. and Nazeem, S., Materials Today: Proceedings, 2 (10) (2015) 5497.

[14] Anila, E.I., Safeera, T.A. and Raman, R., Journal of Fluorescence, 25 (2) (2015) 227.

[15] Zaman, M.B., Chandel, T., Dehury , K. and Rajaram, P., AIP Conference Proceedings, 1953 (1) (2018) 100066.

[16] Falcony, C., Aguilar-Frutis, M.A. and Garcia-Hippolito, M., Micromachines, 9 (414) (2018) 1.

[17] Xiong, H. and Sun, W., Coatings, 7 (207) (2017) 1.

[18] Eid, A.H., Salim, S.M., Sedik, M.B., Omar, H., Dahy, T. and Abou_elkhair, H.M., Journal of Applied Sciences Research, 6 (6) (2010) 777.

[19] Yu, F., Ou, S., Yao, P., Wu, B. and Wuu, D., Journal of Nanomaterials, 594952 (2014) 1.

[20] Padmavathy, V. and Sankar, S., Journal of Materials Science: Materials in Electronics, 29 (2018) 7739.

[21] Zein, R. and Alghoraibi, I., Journal of Nanomaterials, 7541863 (2019) 1.

[22] Ahmed, M., Rasool, K., Imran, Z., Rafiq, M.A. and Hassan, M.M., Saudi International Electronics, Communications and Photonics Conference, Riyadh, Saudi Arabia, IEEE Conference Proceedings, (2011).

[23] Kannappan, P. and Dhanasekaran, R., International Journal of Recent Technology and Engineering, 7 (4s) (2018) 2277.

[24] Bioki, A.H. and Zarandi, M.B., International Journal of Optics and Photonics, 5 (2) (2011) 121.

[25] Offor, P.O., Whyte, G.M., Otung, F.U., Nnamchi, P.S., Ude, S.N., Omah, A.D., Daniel-Npkume, C.C., Neife, S.I., Aigbodion, V.S., Madu, S., Okorie, B.A., Mazza, M. and Ezema, F.I., Surfaces and Interfaces, 16 (2019) 157.

[26] Vishwakarma, R., Journal of Theoretical and Applied Physics, 2015 (9) (2015) 185.

[27] Agbo, P.O., Nwofe, P. and Odo, L.O., Chalcogenide Letters, 14 (8) (2017) 357.

[28] Ebrahimi, S., Yarmand, B. and Naderi, N., Advanced Ceramics Progress, 3 (4) (2017) 3.

[29] Patel, S.B. and Gohel, V.J., Physics and Astronomy International Journal, 1 (4) (2017) 1.

[30] Lanjewar, M., Gohel, J.V., Inorganic and Nano-Metal Chemistry, 47 (7) (2017) 1090.

[31] Gohel, J.V., Jana, A.K. and Singh, M., Applied Physics A, 123 (8) (2017) 1.

[32] Kumari, N., Gohel, J.V. and Patel, S.R., International Journal for Light and Electron Optics, 144 (2017) 422.

[33] Rahman, F., Podder, J. and Ichimura, M., Optik-International Journal of Optics and Photonics, 5 (2) (2011) 79.

[34] Poornima, N., Jose, A., Kartha, C.S. and Vijayakumar, K.P., Procedia-Energy, 15 (2012) 347.

[35] Derbali, A., Attaf, A., Saidi, H., Benamra, H., Nouadji, M., Aida, M.S., Attaf, N. and Ezzaouia, H., Optik-International Journal of Light and Electron Optics, 154 (2018) 286.

[36] Chin, S., Choi, J.W., Woo, H.E., Kim, J.H., Lee, H.S. and Lee, C.L., Nanoscale,11 (13) (2019) 5775.

[37] Mohan, S.R., Joshi, M., Dhami, T., Awasthi, V., Shalu, C., Singh, B. and Singh, V., Synthesis Methods, 224 (2017) 80.

[38] Margoni, M.M., Mathuri, S., Ramamurthi, K., Babu, P.R. and Sethuraman, K., Applied Surface Science, 418 (A) (2017) 280.

[39] Wu, S., Ysng, H., Hu, J., Shen, D., Zhang, H. and Xiao, R., Final Processing Technology, 161 (2017) 162.

[40] Rizk, H.A. and Elanwar, I.M., Canadian Journal of Chemistry, 46 (4) (2011) 507.

[41] Liu, K., Li, J., Xu, Y., Li, H. and Gao, W., Results in Physics, 11 (2018) 749.